

# Eliminating the cuspidal temperature profile of a non-equilibrium chain

Michael M. Cândido and Welles A. M. Morgado  
*Department of Physics, PUC-Rio and  
National Institute of Science and Technology for Complex Systems  
Rua Marquês de São Vicente 225,  
22453-900 Rio de Janeiro — RJ, Brazil*

Sílvio M. Duarte Queirós  
*Centro Brasileiro de Pesquisas Físicas and  
National Institute of Science and Technology for Complex Systems  
Rua Dr Xavier Sigaud, 150,  
22290-180 Rio de Janeiro — RJ, Brazil*

We revisit the 1967 model of heat conduction in a crystal introduced by Z. Rieder, J. L. Liebowitz and E. Lieb. Besides its anomalous heat conduction properties, the model is also characterised by awkward cusps at the ends of the non-equilibrium chain, an effect that has endured the various generalisations of the model. We show that, for a proper combination of the border and bulk pinning values, it is possible to shift from the cuspidal behaviour of the temperature profile to an expected monotonous local temperature evolution along the system. We find a transition regime characterised by a perfect temperature plateau spanning the entire chain (excepting the elements in contact with the reservoirs) separating cuspidal and monotonous behaviour. For each value of the pinning at the border, there are two values of the bulk pinning for which the temperature profile is a straight line. We also relate that change in the temperature profile with both heat transmission and reflection in the chain. Among others, we learn that the first transition — corresponding to the smaller of the two critical edge pinning — takes place when the temperature of the particle connected with the colder reservoir reaches its maximal value as well as the heat flux.

**PACS:**02.50.Ey, 05.10.Gg, 05.60.-k

**Key-words:**Heat fluxes; coupled systems; white noise

## I. INTRODUCTION

The problem of heat conduction is certainly one of the best examples for illustrating the role of statistical mechanics in the treatment of non-equilibrium systems [1–4].

On the one hand, it is a manifestation of the laws of thermodynamics that is synthetically defined by Fourier’s law: the heat flux density is equal to minus the product of the thermal conductivity by the temperature gradient [5].

On the other hand, the discontinuity of matter implies that the macroscopic effects we observe and measure must be related to the way the basic constituents of the systems interact. As early as the introduction of the kinetic theory by Boltzmann, there have been several attempts to microscopically derive and explain the emergence of the Fourier’s law and thereafter the same endeavour was carried out within the context of condensed matter physics [6, 7].

Although the actual microscopic understanding of a physical system requires the application of a quantum mechanical approach, several classical toy models were introduced — especially from the 1950s on — aiming at studying the problem of heat transport in crystals, namely the assumption of chains of linearly coupled oscillators in con-

tact to reservoirs at different temperatures,  $T_1$  and  $T_N$  ( $T_1 < T_N$ ), placed at each end of the chain. Not so surprisingly, these models reach a steady state but do not verify Fourier’s law, *i.e.*, they have an infinite heat conductivity corresponding to ballistic heat transport [8]. To achieve a finite heat conductance in linear systems, that for the homogeneous case can only be truly obtained for higher dimensional non-linear systems [9], several modifications have been introduced [10], from considering mass dispersion [11, 12], extra reservoirs along the chain [13, 14] to effective external collisions [15, 16] among other variations. Nonetheless, when we look at the temperature profile, it is still verified the emergence of a cusp(anticusp) close to the colder(hotter) reservoir, a feature that has not been explained since the introduction of the model by Rieder, Lebowitz and Lieb (RLL) [8], as far as we are aware of.

At first sight, this behaviour is rather odd (the warmer particles are closer to the colder reservoir, and vice versa) and already commented on the abstract of Ref. [8]; we would expect the temperature profile to change monotonously along the chain, even when the bulk temperature is a close to  $\mathcal{T} \equiv (T_1 + T_N)/2$ . Although the RLL model fails to capture the actual behaviour regarding the Fourier law, it is at the origin of a very large num-

ber of heat conduction studies we find in the literature. Moreover, there is still a significant interest in linear chain models [18]; thence, we deem the original model fit to provide answers and further insight into the following questions: *Which are the properties of heat conduction models that induce the (in)famous cuspidal temperature profile? Is it possible to amend this behaviour? In changing the temperature profile to a smooth curve what other modifications are introduced? What does happen to the heat flux as we move from the cuspidal to the smooth temperature profile?* Concerning the first question, we slightly lift the veil to say that this behaviour stems from the pinning conditions of the model. The real impact of the pinning conditions in the temperature profile and the answers to the remaining questions will be presented hereinafter and constitute the main goal of this manuscript.

Explicitly, we propose an explanation for the behavior of the local temperature profile, which goes from the expected monotonous increase from the cold side of the chain towards the hot side to a quite unexpected cusp-like behavior where the temperatures of the half-chain closer to the cold reservoir are hotter than the local temperatures of the other half-chain, closer to the hot reservoir. As we found out, the factors that drive this intriguing transition are the pinning intensity (bulk and surface), the thermal conductance of the chain, and the temperatures of the first and second (also the  $N - 1$ -th and  $N$ -th) particles.

## II. MODEL AND RESULTS

Our study revolves around the dynamics of a chain of  $N$  linearly coupled oscillators ruled by the set of equations,

$$\begin{cases} m \frac{d^2 x_1}{dt^2} = -\gamma \frac{dx_1}{dt} - k' x_1 - k_1 (x_1 - x_2) + \eta_1 \\ m \frac{d^2 x_i}{dt^2} = -k x_i - k_1 (2x_i - x_{i+1} - x_{i-1}) \\ m \frac{d^2 x_N}{dt^2} = -\gamma \frac{dx_N}{dt} - k' x_N - k_1 (x_N - x_{N-1}) + \eta_N \end{cases} \quad (1)$$

( $2 \leq i \leq N - 1$ ), where  $\eta$  is Gaussian distributed with,

$$\langle \eta_i(t) \eta_j(t') \rangle = 2\gamma T_i \delta_{ij} \delta(t - t'), \quad (2)$$

with  $T_i$  representing the temperature of each reservoir ( $i, j = \{1, N\}$ ). Our analytical approach is made using a Stratonovich interpretation of the noise. The seminal model treated by Rieder, Lebowitz and Lieb corresponds to the specific case  $k = 0$  and  $k_1 = k'$ .

Traditionally, the solution to the problem is carried out assuming a multivariate Fokker-Planck treatment, particularly by making use of the eigenvalue approach [17]. In this manuscript, we handle the problem differently; instead of moving into the probability space and using such methods, we perform our calculations in the Fourier-Laplace space [19]. Explicitly, for the position, we have,

$$\tilde{x}(iq + \varepsilon) \equiv \int_0^\infty x(t) e^{-(iq + \varepsilon)t} dt, \quad (3)$$

and for the velocity [considering  $x_i(0) = 0$  and  $v_i(0) = 0$  for all  $i$  without any loss of generality],

$$\tilde{v}(iq + \varepsilon) = (iq + \varepsilon) \tilde{x}(iq + \varepsilon). \quad (4)$$

As usual, we consider that the system is in local equilibrium and the temperature at site  $i$ ,  $\mathcal{T}_i$ , is established by the canonical relation,

$$\mathcal{T}_i \equiv m \langle v_i^2 \rangle. \quad (5)$$

The equations of motion in Eq. (1) can be recast in the form,

$$\mathcal{D}(t) \mathbf{x}(t) = \boldsymbol{\eta}(t), \quad (6)$$

where  $\mathcal{D}(t)$  is a  $N \times N$  operator,  $\mathbf{x}(t)$  is the vector of the positions,  $\mathbf{x}(t) \equiv \{x_1(t), \dots, x_N(t)\}$  and  $\boldsymbol{\eta}(t) \equiv \{\eta_1(t), 0, \dots, 0, \eta_N(t)\}$  represents the multivariate stochastic variable describing the fluctuations introduced by the reservoirs. Fourier-Laplace transforming Eq. (6) we get,

$$\tilde{\mathcal{D}}(iq + \varepsilon) \tilde{\mathbf{x}}(iq + \varepsilon) = \tilde{\boldsymbol{\eta}}(iq + \varepsilon) \quad (7)$$

$$\tilde{\mathbf{x}}(iq + \varepsilon) = \tilde{\mathcal{A}}(iq + \varepsilon) \tilde{\boldsymbol{\eta}}(iq + \varepsilon), \quad (8)$$

where  $\mathcal{A} \equiv \mathcal{D}^{-1}$ . From Eq. (8) the position of particle  $i$  yields,

$$\tilde{x}_i(iq + \varepsilon) = \sum_{j=1, N} \tilde{\mathcal{A}}_{ij}(iq + \varepsilon) \tilde{\eta}_j(iq + \varepsilon), \quad (9)$$

and the noise in the reciprocal space,  $\tilde{\eta}$ , is still Gaussian with,

$$\langle \tilde{\eta}_i(iq_1 + \varepsilon) \tilde{\eta}_j(iq_2 + \varepsilon) \rangle = \frac{2\gamma T_i}{iq_1 + iq_2 + 2\varepsilon} \delta_{ij}. \quad (10)$$

In this non-equilibrium problem, we are mainly interested in the steady state properties where the

<sup>1</sup> The forms of the both operators are made explicit in the appendix.

ergodic equivalence between statistics over samples and statistics over time holds. To benefit from the Fourier-Laplace representation, instead of performing the standard averaging in time of a stationary random function  $f$ ,

$$\bar{f} \equiv \lim_{\Xi \rightarrow \infty} \frac{1}{\Xi} \int_0^{\Xi} f(t) dt, \quad (11)$$

we resort to the final value theorem which states that [20],

$$\bar{f} = \lim_{z \rightarrow 0} z \int_0^{+\infty} \exp[-zt] f(t) dt \quad (12)$$

$$= \lim_{z \rightarrow 0, \varepsilon \rightarrow 0} \int_{-\infty}^{+\infty} \frac{dq}{2\pi} \frac{z}{z - (iq + \varepsilon)} \tilde{f}(iq + \varepsilon) \quad (13)$$

where the Fourier-Laplace representation of  $f(t)$  was used.

Plugging Eqs. (5) and (4) into (13) we obtain,

$$\mathcal{T}_i = m \lim_{z \rightarrow 0, \varepsilon \rightarrow 0} \int_{-\infty}^{+\infty} \frac{dq_1 dq_2}{2\pi} \frac{z}{z - (iq_1 + iq_2 + 2\varepsilon)} \times \langle \tilde{v}_i(iq_1 + \varepsilon) \tilde{v}_i(iq_2 + \varepsilon) \rangle. \quad (14)$$

After some algebra based on the property given by Eq. (10), we get the final expression,

$$\mathcal{T}_i = \frac{m\gamma}{\pi} \sum_{j=1, N} T_j \int_{-\infty}^{+\infty} q^2 \tilde{\mathcal{A}}_{ij}(iq + \varepsilon) \tilde{\mathcal{A}}_{ij}(-iq - \varepsilon) dq. \quad (15)$$

### A. Transition in the temperature profile

As we have mentioned and originally found in Ref. [8], when the bulk elements of the chain are unpinned,  $k = 0$  (and  $k' = k_1$ ), the temperature profile is that with the cusp starting at site  $i = 2$  and the anti-cusp ending at site  $i = N - 1$  (see left-hand panel in Fig. 1). The absolute deviation of the canonical temperature  $\mathcal{T}_i$  from  $(T_1 + T_N)/2$  is known to follow an exponential decay with the distance of the site  $i$  and one of the ends (see the dashed blue line in Fig. 2).

Introducing the pinning for the elements of the bulk — *e.g.*, by the interaction between the whole chain with the substrate — the (anti)cusps get smoother and, for a critical value  $k_{\text{crit}} \equiv k_{\text{crit}}(k', k_1)$ , yield an exact temperature plateau at  $\mathcal{T}$  for all particles [except  $i = (1, N)$ ] (see central panel in Fig. 1). According to our analysis the critical pinning of the bulk follows the size-independent relation,

$$k_{\text{crit}_1} = \frac{(k' + k_1)}{4}, \quad (k' = k_1). \quad (16)$$

As we continue increasing the pinning of the bulk, the plateau is destroyed and a non-cuspidal temperature profile in the chain is observed (see right-hand panel in Fig. 1). In this case, we verify the same exponential decay of the deviation as a function of the distance to the respective ends (see the full red line Fig. 2).

In Fig. 3, we depict the typical evolution of the temperature of the second particle (the first bulk particle) with respect to  $k$  (bulk pinning). For  $k > k_{\text{crit}}$ , the  $i = 2$  particle's local temperature will approach the temperature  $\mathcal{T}$  from below.

Let us shed some light on this phenomenon by having a closer look at the temperatures of the second and penultimate particles  $\mathcal{T}_2$  and  $\mathcal{T}_{N-1}$ , respectively. Because they are those which drive the behaviour of the temperature of the remaining bulk particles we shall call them guiding temperatures (GT). Several factors combine to set the values of GT, the most important being the thermal conductance of the system and the temperature of the neighbours, in special those of the particles closest to the reservoirs,  $\mathcal{T}_1$  and  $\mathcal{T}_N$ . Intuitively, increasing the pinning at the edges, we would insulate particles 1 and  $N$  from the bulk and make the canonical temperatures  $\mathcal{T}_1$  and  $\mathcal{T}_N$  approach the temperature of the reservoirs  $T_1$  and  $T_N$ .

Enlarging the space of parameters by loosening the condition  $k' = k_1$ , we find two transitions. Increasing  $k'$  from zero, for a given pair of values  $(k, k_1)$ , we find a first transition from monotonous to cuspidal behaviour of the profile and afterwards a second change to a monotonous profile as depicted in Fig. 5. For the second transition we deduced the relation,

$$k'_{\text{crit}_2} = k + k_1 + \frac{\gamma^2}{m}, \quad (17)$$

whereas for the first transition,  $k'_{\text{crit}_1}$ , we could only find the respective critical line, as plotted in Fig. 4, by a numerical procedure. It is worth stressing that all the other results we present in this manuscript are obtained *analytically*.

Early studies on Lyapunov exponents of thermal conductivity models [21], namely the Toda model [22] and the ding-a-ling model [23] have pointed to a critical-like behaviour with finite-size effects. In our case, we tested the critical relations in chains of different sizes and we have found no sensitiveness to the size of the system.

### B. Maximal heat transmission

The temperature profile characterising the non-equilibrium condition of the chain is the outcome

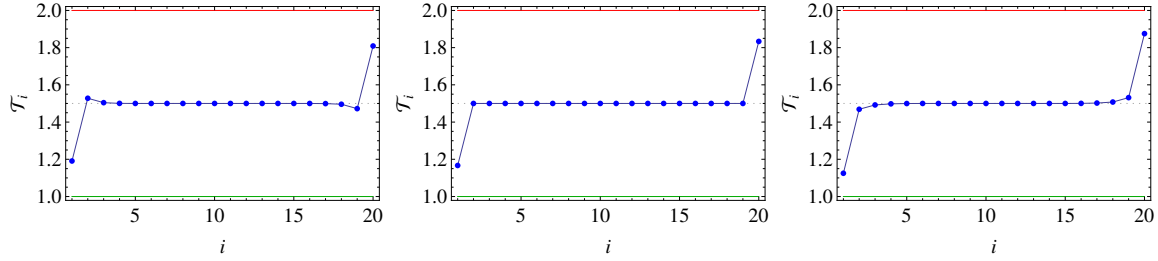


FIG. 1. Temperature profile of a chain governed by Eq. (1) with  $m = 1$ ,  $\gamma = 1$ ,  $k' = k_1 = 1$ . Left: The RLL case with  $k = 0$ ; centre: the critical case  $k = k_{crit} = 1/2$ ; right: a typical smooth profile for  $k = 1$ .

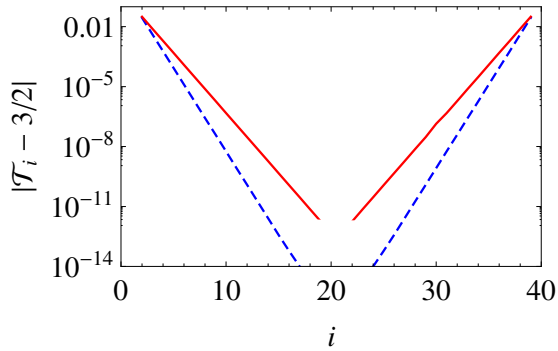


FIG. 2. Absolute deviation from the plateau temperature versus site position in log-linear scale. The blue dashed line is for the cuspidal RLL situation  $k' = k_1 = 1$  and  $k = 0$ , whereas the red line represents the normal case with  $k = 1$ .

of its mechanical features that define the heat flux along the system. To describe it, we center attention on the average flux from the reservoir onto particle  $i = 1$  (the colder particle),

$$\mathcal{J} = \lim_{z \rightarrow 0} z \int \exp[-zt] \langle \eta_1(t) v_1(t) - \gamma v_1^2(t) \rangle, \quad (18)$$

that combined with a Fourier-Laplace description of the dynamics has been used to describe the conductance in (non-linear) thermal and athermal problems [24]. Using Eq. (8) and the relation,  $\bar{v}(iq + \varepsilon) = (iq + \varepsilon) \tilde{x}(iq + \varepsilon)$ , we recast the last equation in reciprocal space into,

$$\mathcal{J} = \gamma^2 \frac{\Delta T}{\pi} \int (iq + \varepsilon)^2 \tilde{\mathcal{A}}_{1N}(iq + \varepsilon) \tilde{\mathcal{A}}_{1N}(-iq - \varepsilon) dq, \quad (19)$$

with  $\Delta T \equiv T_N - T_1$ .

By scanning the  $(k, k', k_1)$  sub-space of parameters, and analyzing the dependence of the flux  $\mathcal{J}$  on them, we verified that our previous argument on the behaviour between the canonical temperature at the edges is only partially correct (please follow it from Fig. 5). As a matter of fact, that qualitative

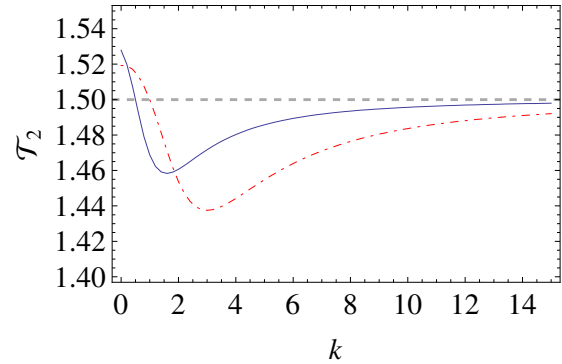


FIG. 3. Canonical temperature of the second particle of the chain,  $\mathcal{T}_2$ , vs bulk pinning,  $k$ , with  $m = 1$ ,  $\gamma = 1$ . The full blue line is for  $k' = k_1 = 1$  and red dot-dashed line is for  $k' = k_1 = 2$ . The critical values of  $k$  are  $k_{crit} = 1/2$  and  $k_{crit} = 1$ , respectively, and concur with Eq. (16). For large values of the coupling,  $k \rightarrow \infty$ , the chain turns into an incompressible wire and the canonical temperature naturally approaches  $3/2$ .

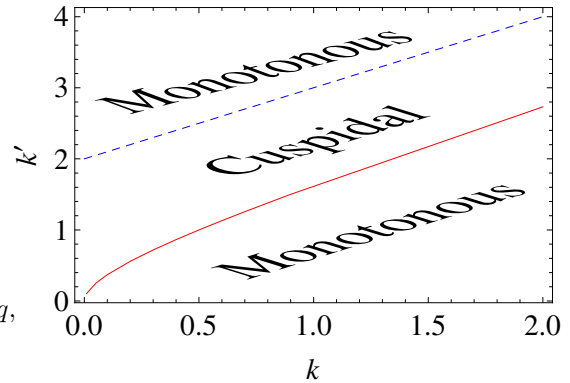


FIG. 4. Critical lines defining different behaviour for  $k_1 = 1$ . The red line indicates the first plateau,  $k_{crit1}$ , and the blue dashed line is given by Eq. (17). Both lines appear to run parallelly for large values of  $k$ .

relation only holds after  $k'$  reaches the first critical value corresponding to the first plateau. That is to say, there is a first regime wherein the increasing of the pinning of the edge particles enhances the thermal conductivity in the chain as though inserting an adequate snag in the chain favours the heat flux instead of hampering it. Accordingly, when the flux is maximal the temperature  $\mathcal{T}_1$  ( $\mathcal{T}_N$ ) reaches its maximal (minimal) value. However, the temperature  $\mathcal{T}_2$  ( $\mathcal{T}_{N-1}$ ) keeps on increasing (decreasing) its value with the pinning  $k'$ , thus giving rise to the unusual, and counterintuitive, temperature profile between the critical plateaux. With this observation in mind we are inclined to consider that anomalous behaviour as a sort of overshoot (undershoot) — characterised by the cusp and anticusp — that after the second plateau turns into a negative overshoot(undershoot) before finally relaxing to the  $\mathcal{T} = 3/2$  behaviour.<sup>2</sup>

### III. CONCLUDING REMARKS

In this manuscript we studied a generalization of a well known model of a harmonic chain in contact with two heat reservoirs with different temperatures  $T_1$  and  $T_N$  ( $T_1 < T_N$ ). The model is known to bear a ballistic regime of heat transmission with the temperature profile close to a plateau with a cusp(anticusp) close to the colder(hotter) reservoir. That profile is reckoned odd since it makes the half of the bulk particles sitting closer to the colder reservoir hotter than the other half of the bulk particles that are sitting next to the hotter reservoirs! By adjusting the pinning value at the edges of the chain we were capable of transitioning between cuspidal and monotonous behaviour. That transition is characterised by the emergence of a temperature plateau with  $\mathcal{T}_i = (T_1 + T_N)/2$  (for all  $2 \geq i \geq N-1$ ). Fixing the value of the pinning in the bulk and the value of the coupling constant we identified the two of these plateaux. For the second we managed to infer a relation between all the mechanical parameters of the problem.

In further analysing the thermal properties of the chain, we found that the first plateau is associated with a maximal(minimal) value of the first(last) particle. Thus, to some extent, when we introduce some sort of hurdle — in our case the pinning  $k'$  — we end up homogenizing the behaviour of the particles at the edge with those in

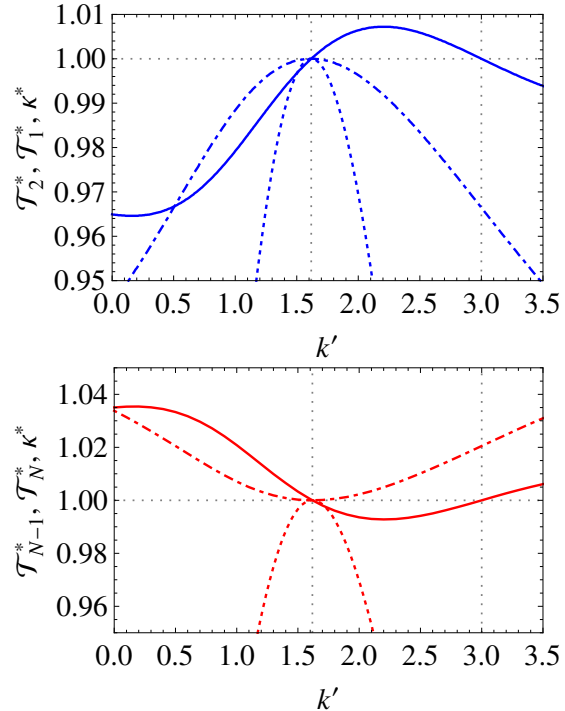


FIG. 5. Upper panel: Normalised values of the canonical temperatures  $\mathcal{T}_1$  (dotted-dashed line),  $\mathcal{T}_2$  (full line) and conductance  $\kappa$  (dotted line) vs edge pinning,  $k'$ , with  $m = 1$ ,  $\gamma = 1$  and  $k = k_1 = 1$ . Both  $\mathcal{T}_1$  and  $\kappa$  are normalised by the respective maximal values whereas  $\mathcal{T}_2$  is normalised by the critical value  $\mathcal{T} = 3/2$ . The three lines intersect at the critical plateau value  $k'_{crit1} = 1.618033988749894\dots$  with value 1 for all of the three quantities. Lower panel: Normalised values of the canonical temperatures  $\mathcal{T}_N$  (dotted-dashed line),  $\mathcal{T}_{N-1}$  (full line) and conductance  $\kappa$  (dotted line) vs edge pinning,  $k'$ , with  $m = 1$ ,  $\gamma = 1$  and  $k = k_1 = 1$ . Temperature  $\mathcal{T}_N$  is normalised by its minimal value,  $\kappa$  by its maximal values whereas  $\mathcal{T}_{N-1}$  is normalised by the critical value  $\mathcal{T} = 3/2$ . Again, the three lines still intersect at the same critical plateau value  $k'_{crit2}$  with value 1 for all of the three quantities. The temperatures  $\mathcal{T}_2$  and  $\mathcal{T}_{N-1}$  equal the critical value once again for  $k'_{crit2} = 3$  as given by Eq. (17) and both temperatures approach the value  $3/2$  as  $k' \rightarrow \infty$ .

the bulk. As we go on increasing that pinning, we get the opposite effect, the particles at the edge of the chain become increasingly different from the others and thus they thwart the transmission of heat along the system.

There are some features of the particle temperature that are crucial for the understanding of the cuspidal behaviour. The first one is the behaviour of the temperature of the particles that are in contact with the reservoirs,  $\mathcal{T}_1$  and  $\mathcal{T}_N$ . The thermal conductance initially increases as we increase the surface pinning (bulk pinning fixed) and reaches

<sup>2</sup> Phenomena of overshooting appear in a variety of physical systems. For instance, the entropy production of the logistic map surpasses its expected value before approaching it from above (see for instance Ref. [25]).

a peak decreasing monotonically after that. We know that the higher the thermal conductance the higher is the thermal contact of the extremities with the bulk. That makes the former closer in value to the bulk temperatures. Therefore, the peak of thermal conductivity should correspond to the smallest difference between the temperatures of 1 (and  $N$ ) and that of the bulk. This is seen in Fig. 5 where the peaks of  $\mathcal{T}_1$  and the thermal conductivity concur at the same point, but with the peak of conductance being a sharper than that of  $\mathcal{T}_1$ .

Another important point is the differences  $\mathcal{T}_2 - \mathcal{T}_1$  and  $\mathcal{T}_N - \mathcal{T}_{N-1}$ . The GT are influenced by the values of the temperatures of the extremities (ToE). If all other factors were kept constant, the value of the GT would increase or decrease as the ToE. Although we did not manage to find a sound reason the conductance and  $\mathcal{T}_1$  reach maximal values for the same  $k'$  the temperature profile exhibits an exact plateau, the increase of  $\mathcal{T}_2$  might probably be due to the sharper decrease in conductivity (less transmitted heat from 2 to 1 should help increase  $\mathcal{T}_2$ , or decrease  $\mathcal{T}_{N-1}$  on the other side of the lattice) then the decrease of  $\mathcal{T}_1$  (which has the effect of decreasing  $\mathcal{T}_1$ ).

As we further increase  $k'$ ,  $\mathcal{T}_2$  increases up to a maximum and then it starts to decrease until it reaches the average  $(T_1 + T_2)/2$  again at the second critical value (at this point the bulk temperatures form again an exact plateau at  $(T_1 + T_2)/2$ ). For larger values of  $k'$ ,  $\mathcal{T}_2$  decreases down to a minimum, probably driven mostly by the decrease of  $\mathcal{T}_1$ . However, for even larger  $k'$ , the conductance keeps decreasing monotonically and that makes the particles 1 and  $N$  ever more insulated from the bulk ones. Indeed, the higher the  $k'$ , the less the

particle 2 will be influenced by particle 1 since the last one is free to physically move very little. Any further increase in the value  $k'$  will only bring  $\mathcal{T}_2$  and the rest of the bulk temperatures monotonically closer to the average  $(T_1 + T_2)/2$ . In fact, for very large  $k'$ , the system behaves as an almost trapping box for the phonons, leading to complete thermalization at the average temperature  $(T_1 + T_2)/2$ .

In summary, by increasing the surface pinning coupling  $k'$ , the local temperature distribution for the particles goes from monotonous to cuspidal, and to monotonous again. It might be possible that a similar qualitative behaviour of transitions between cuspidal and monotonous temperature profiles, depending on the values of the mechanical parameters, would also be present in RLL-inspired models yielding a finite heat conductance (Fourier law), namely non-linear, higher dimensional coupling models. The probing of that hypothesis as well as a further analysis about higher-order statistics are addressed for future work.

## ACKNOWLEDGMENTS

We would like to thank the partial funding from FINEP [contract No. PUC-Infra 1580/10], FAPERJ [contract No. APQ1-110.635/2014] and CNPq [contract No.s 481640/2011-8 and 308737/2013-0].

## APPENDIX: MATRIX FOR $\mathcal{D}(s)$ AND $\mathcal{A}(s)$

The matrix of dynamics,  $\mathcal{D}(s)$ , in Laplace space is written as:

$$\mathcal{D}(s) =$$

$$= \begin{pmatrix} ms^2 + \gamma s + k_1 + k' & -k_1 & \cdots & \cdots & \cdots & 0 \\ -k_1 & ms^2 + 2k_1 + k & -k_1 & \cdots & \cdots & 0 \\ 0 & -k_1 & \cdots & \cdots & \cdots & 0 \\ \vdots & \vdots & \ddots & -k_1 & \cdots & 0 \\ \vdots & \vdots & \vdots & \ddots & \cdots & 0 \\ \vdots & \vdots & \vdots & \ddots & \cdots & 0 \\ 0 & \cdots & 0 & -k_1 & ms^2 + 2k_1 + k & -k_1 \\ 0 & \cdots & 0 & 0 & -k_1 & ms^2 + \gamma s + k_1 + k' \end{pmatrix}$$

And its inverse is:

$$\mathcal{A}(s) =$$

$$= \begin{pmatrix} A_{11}(s) & A_{12}(s) & A_{13}(s) & \cdots & \cdots & A_{1N}(s) \\ A_{21}(s) & A_{22}(s) & A_{32}(s) & \cdots & \cdots & A_{2N}(s) \\ \vdots & \vdots & \ddots & \cdots & \cdots & \vdots \\ \vdots & \vdots & \vdots & \ddots & \cdots & \vdots \\ \vdots & \cdots & \cdots & \cdots & \ddots & \vdots \\ A_{N1}(s) & \cdots & \cdots & \cdots & \cdots & A_{NN}(s) \end{pmatrix}$$

The elements  $\mathcal{A}(s)_{ij}$  has the structure:

$$\mathcal{A}(s)_{ij} = \frac{a_0 + a_1 s + a_2 s^2 + \dots + a_{2n-3} s^{2n-3} + a_{2n-2} s^{2n-2}}{\text{Det}[\mathcal{D}(s)]}$$

Where  $n$  represents the dimension of the chain, and the  $a_k$  are different constants for each  $\mathcal{A}(s)_{ij}$ .

Taking the particular case  $N = 4$  and using the parameters  $k' = k = k_1 = \gamma = m = 1$ ,  $\mathcal{D}(s)$  and  $\mathcal{A}(s)$  are written, respectively, as:

$$\mathcal{D}(s) = \begin{pmatrix} s^2 + s + 2 & -1 & 0 & 0 \\ -1 & s^2 + 3 & -1 & 0 \\ 0 & -1 & s^2 + 3 & -1 \\ 0 & 0 & -1 & s^2 + s + 2 \end{pmatrix}$$

$$\mathcal{A}(s) = \frac{1}{\text{Det}[\mathcal{D}(s)]} \times \begin{pmatrix} \mathcal{A}(s)_{11} & \mathcal{A}(s)_{12} & \mathcal{A}(s)_{13} & \mathcal{A}(s)_{14} \\ \mathcal{A}(s)_{21} & \mathcal{A}(s)_{22} & \mathcal{A}(s)_{23} & \mathcal{A}(s)_{24} \\ \mathcal{A}(s)_{31} & \mathcal{A}(s)_{32} & \mathcal{A}(s)_{33} & \mathcal{A}(s)_{34} \\ \mathcal{A}(s)_{41} & \mathcal{A}(s)_{42} & \mathcal{A}(s)_{43} & \mathcal{A}(s)_{44} \end{pmatrix}$$

Where  $\text{Det}[\mathcal{D}(s)]$  is:

$$\text{Det}[\mathcal{D}(s)] = s^8 + 2s^7 + 11s^6 + 16s^5 + 40s^4 + 38s^3 + 54s^2 + 26s + 21$$

And for entries we have:

$$\mathcal{A}(s)_{11} = \mathcal{A}(s)_{44} = s^6 + s^5 + 8s^4 + 6s^3 + 19s^2 + 8s + 13$$

$$\mathcal{A}(s)_{12} = \mathcal{A}(s)_{43} = s^4 + s^3 + 5s^2 + 3s + 5$$

$$\mathcal{A}(s)_{13} = \mathcal{A}(s)_{42} = 2 + s + s^2$$

$$\mathcal{A}(s)_{14} = \mathcal{A}(s)_{41} = 1$$

$$\mathcal{A}(s)_{21} = \mathcal{A}(s)_{34} = s^4 + s^3 + 5s^2 + 3s + 5$$

$$\mathcal{A}(s)_{22} = \mathcal{A}(s)_{33} = s^6 + s^5 + 8s^4 + 6s^3 + 19s^2 + 8s + 13$$

$$\mathcal{A}(s)_{23} = \mathcal{A}(s)_{32} = s^4 + 2s^3 + 5s^2 + 4s + 4$$

$$\mathcal{A}(s)_{24} = \mathcal{A}(s)_{31} = 2 + s + s^2$$

- 
- [1] H. Nakazawa, Prog. Theor. Phys. Supp. **45** 231 (1970).  
 [2] S. Lepri, R. Livi and A. Politi, Phys. Rep. **377** 1 (2003).  
 [3] A. Dhar, Adv. Phys. **57** 457 (2008).  
 [4] F. Bonetto, J. L. Lebowitz and L. Rey-Bellet, *Mathematical Physics 2000* edited by A. Fokas,

- A. Grigoryan, T. Kibble and B. Zegarlinsky (Imperial College Press, London, 2000), page 128.  
 [5] R. Kubo, M. Toda and N. Hashitsume, *Statistical Physics II: Nonequilibrium Statistical Mechanics* (Springer, Berlin, 1991).  
 [6] N. W. Ashcroft and N. D. Mermin, *Solid State Physics* (Rinehart and Winston, New York, 1976).

- [7] P. M. Chaikin and T. C. Lubensky, *Principles of Condensed Matter Physics* (Cambridge University Press, Cambridge, 1995).
- [8] Z. Rieder, J. L. Lebowitz and E. Lieb, *J. Math. Phys.* **8** 1073 (1967).
- [9] K. Saito and A. Dhar, *Phys. Rev. Lett.* **104** 040601 (2010).
- [10] V. Kannan, *Heat Conduction in Low Dimensional Lattice Systems* (Ph.D. Dissertation, School-New Brunswick Rutgers, The State University of New Jersey, 1995).
- [11] J. P. Huang and K. W. Yu, *Phys. Rep.* **431** 87 (2006).
- [12] N. Yang, N. Li, L. Wang and B. Li, *Phys. Rev. B* **76** 020301(R) (2007).
- [13] S. Lepri, R. Livi and A. Politi, *Europhys. Lett.* **43** 271 (1998).
- [14] F. Bonetto, J. L. Lebowitz and J. Lukkarinen, *J. Stat. Phys.* **116** 783 (2004).
- [15] A. Dhar, K. Venkateshan and J. L. Lebowitz, *Phys. Rev. E* **83** 021108 (2011).
- [16] G. T. Landi and M. J. de Oliveira, *Phys. Rev. E* **89** 022105 (2013).
- [17] P. G. Bergmann and J. L. Lebowitz, *Phys. Rev.* **99** 578 (1955).
- [18] see for instance: V. Kannan, A. Dhar and J. L. Lebowitz, *Phys. Rev. E* **85** 041118 (2012); J. D. Bodyfelt, M. C. Zheng, R. Fleischmann and T. Kottos, *Phys. Rev. E* **87** 020101(R) (2013); G. T. Landi and M. J. de Oliveira, *Phys. Rev. E* **89** 022105 (2014); D. Lacoste and M. A. Lomholt, *Phys. Rev. E* **91** 022114 (2015).
- [19] D. O. Soares-Pinto and W. A. M. Morgado W. A. M., *Physica A* **365** 289 (2006).
- [20] B. van der Pol and H. Bermmmer H., *Operational Calculus Based on the Two-Sided Laplace Integral* (Cambridge University Press, Cambridge, 1950).
- [21] D. J. R. Mimmagh, *Thermal conductivity and dynamics of a chain of free and bound particles* (Ph.D. Dissertation, Simon Fraser University, 1997).
- [22] M. Toda, *J. Phys. Soc. Japan* **22** 431 (1967).
- [23] G. Casati, J. Ford, F. Vivaldi and W. M. Visscher, *Phys. Rev. Lett.* **52** 1861 (1984).
- [24] D. O. Soares-Pinto and W. A. M. Morgado, *Phys. Rev. E* **77** 011103 (2008); W. A. M. Morgado and D. O. Soares-Pinto, *Phys. Rev. E* **79** 051116 (2009); W. A. M. Morgado and S. M. Duarte Queirós, *Phys. Rev. E* **86** 041108 (2012); W. A. M. Morgado and S. M. Duarte Queirós, *Phys. Rev. E* **90** 022110 (2014).
- [25] H. Gould and J. Tobochnik, *An Introduction to Computer Simulation Methods: Applications to Physical System* 2nd Ed. (Addison-Wesley, Reading - MA, 1995).